Desalination and Water Treatment
www.deswater.com

doi: 10.5004/dwt.2023.29451

289 (2023) 197–205
March

Inhibition performance of benzotriazole-based composite inhibitor against carbon steel corrosion in stone processing wastewater

Jingjing Xiang[a], Hao Peng[a], Likun Li[b,*], Heng Liu[a], Qiaoyun Zhu[a], Yanjun Huang[a], Yi Wang[a], Guozhi Fan[a], Lei Zhang[a,*]

[a]*School of Chemistry and Environmental Engineering, Wuhan Polytechnic University, Wuhan 430023, China, emails: zhanglei@whpu.edu.cn (L. Zhang), 1511621536@qq.com (J. Xiang), 119064337@qq.com (H. Peng), wh18271843987@163.com (H. Liu), 1930087696@qq.com (Q. Zhu), hyj.321@163.com (Y. Huang), wangyi2020@whpu.edu.cn (Y. Wang), fgzcch@whpu.edu.cn (G. Fan)*
[b]*China-Ukraine Institute of Welding, Guangdong Academy of Sciences, Guangzhou 510650, China, email: lilk@gwi.gd.cn (L. Li)*

Received 23October 2022; Accepted 1 March 2023

ABSTRACT

The cutting saw blade with diamond blade and carbon steel matrix is widely used in stone cutting because of its high strength, impact resistance and good thermal stability. However, the carbon steel matrix is easy to corrode in the circulating cooling water, which shortens its service life. In this study, a new highly efficient benzotriazole-based (BMN) composite inhibitor was synthesized and investigated against the corrosion of carbon steel in stone processing wastewater. The corrosion inhibition properties and mechanism of prepared BMN for carbon steel in real stone processing wastewater were evaluated and deduced using the experimental weight loss, electrochemical and surface morphology characterization techniques. Weight loss methods results showed that a high inhibition efficiency of 99.59% in stone processing wastewater was achieved at ambient temperature, with the stirring speed 200 rpm, the immersion time 7 d, and the BMN concentration is 50 mL·L^{-1}. Electrochemical impedance spectroscopy indicated that resistance from the surface films (R_2) and charge transfer resistance (R_3) were enhanced with increase in BMN concentration. Polarisation results revealed the BMN acted as an anodic inhibitor, owing to the addition of BMN resulted in the significant change of anodic Tafel slopes (β_a). Scanning electron microscopy results indicated BMN formed a protective film on the surface of carbon steel through adsorption. In short, the prepared BMN composite inhibitor exhibited superior anti-corrosion performance for saw blade corrosion in stone processing wastewater, which had great application potential in industries.

Keywords: Stone processing wastewater; Benzotriazole; Corrosion inhibitor; Electrochemical tests; Corrosion mechanism

1. Introduction

The open circulating water cooling system is used to cool the saw blade cutting marble in the process of stone processing. And at this time, the cooling water containing suspended solids, anions and cations constantly corrodes the saw blade, shortens equipment lifespan and causes huge economic losses [1–3]. Therefore, it is of great significance to explore the anti-corrosion characteristics of carbon steel saw blade in high-salinity wastewater [4]. Currently, there are many methods to protect metal surface against corrosion, such as using corrosion-resistant steel, coating and adding corrosion inhibitor, and so forth [5,6]. Among these methods, the use of inhibitors is considered to be the most economical strategy, which can effectively reduce or delay the metal corrosion process [6–8]. At present, most commercially

* Corresponding authors.

available corrosion inhibitors such as, carboxylic acid organic corrosion inhibitors, are relatively inexpensive, but the corrosion inhibition performance is weak [9]. On the contrary, most of the traditional corrosion inhibitors contain organic phosphoric acid. A large amount of untreated phosphorus-containing water will lead to algae growth, resulting in eutrophication of the water body, harming the water environment, and increasing the cost of water treatment [10,11]. Therefore, it is important to develop a kind of corrosion inhibitor with low price and excellent performance that can meet the large-scale use of stone processing plants.

Most inhibitors retard metal corrosion by forming an inhibition layer on the metal surface through adsorption [8]. Benzotriazole (BTA), an effective organic corrosion inhibitor that has been studied for many years [12,13]. However, the corrosion inhibition effect of single BTA is poor and expensive [14]. It has been turned out that a cost-effective strategy is to utilize the synergistic effect of the corrosion inhibitor, which can reduce the amount of a single reagent and improve the corrosion inhibition effect. The MoO_4^{2-} exhibits a superior anticorrosion performance, and molybdenum is low in toxicity and has a low degree of environmental pollution, which is generally used in synergy with corrosion inhibitors such as BTA [15,16]. Nitrite is an effective metal corrosion inhibitor, usually used together with sodium benzoate and other corrosion inhibitors, which has good corrosion inhibition effect and can form an oxide film on the metal surface [17,18]. Sodium benzoate, as an anode type corrosion inhibitor, can form a protective film on the metal surface by adsorption [19]. Silicate has been widely used as corrosion inhibitor, as a result of its great attractiveness in terms of non-toxicity and low cost. Moreover, silicates were usually employed with organic inhibitor to accelerate the film formation. Liu et al. [20], Wang et al. [21] and Coelho et al. [22] reported that silicate could form an insoluble film on the surface of the metal through electrostatic adsorption to inhibit the cathode and anode reactions of the metal. This work will present an innovative idea to use BMN as an effective corrosion inhibitor to inhibit the corrosion of saw blade for carbon steel in stone processing wastewater.

2. Materials and methods

2.1. Materials

Benzotriazole (BTA, CP), sodium nitrite ($NaNO_2$), triethanolamine ($C_6H_{15}NO_3$), sodium molybdate dihydrate ($Na_2MoO_4{\cdot}2H_2O$) were purchased from Sinopharm Chemical Reagent Co., Ltd., (China). Sodium benzoate (C_6H_5COONa) was supplied from Chengdu Cologne Chemicals Co., Ltd., (China). Sodium silicate ($Na_2SiO_3{\cdot}9H_2O$) was procured from Shanghai Lingfeng Chemical Reagent Co., Ltd., (China). Sodium nitrite, triethanolamine, sodium molybdate dihydrate, sodium benzoate and sodium silicate are all analytically pure. All chemical reagents were used as received without further separation and purification. Deionized water (18.2 MΩ·cm) was used throughout the experiments.

To investigate the corrosion inhibition of BMN in stone processing wastewater, A3 carbon steel coupons were used in this study. The A3 carbon steel coupons in the form of cubes with sizes 50 mm × 25 mm × 2 mm were investigated. Stone processing wastewater was provided by a stone processing factory in Macheng (China) as a corrosive medium. Table 1 shows the characteristics of the stone processing wastewater.

2.2. Preparation of BMN composite inhibitor

Firstly, $Na_2SiO_3{\cdot}9H_2O$, triethanolamine and sodium benzoate were mixed at a mass ratio of 3:4:10 in a three-necked flask (i.e., 0.6 g:0.8 g:2.0 g in a 250 mL flask). 100 mL of deionized water was added to the flask as a solvent, and the mixture was stirred and heated in a water bath at 30°C–40°C for 10 min. Secondly, $NaNO_2$, $Na_2MoO_4{\cdot}2H_2O$ and BTA were added to the three-necked flask (3 g:0.6 g:0.04 g), then the reaction mixture was continued to stir in the water bath until completely dissolved. Finally, deionized water was poured into the flask and stirred for 2~3 min at room temperature and the volume ratio of deionized water to the mixed solution is 2:1.

2.3. Weight loss methods

A3 carbon steel coupons were polished and cleaned to avoid the influence of surface condition. The A3 carbon steel coupons were first polished by using abrasive paper #240, #400, #1000, #1200 and #1500 in sequence, then cleaned with deionized water and finally degreased with ethanol and acetone. The prepared A3 carbon steel coupons were dried and soaked in BMN composite inhibitor solution for 3–5 min, then dried and weighed under room temperature conditions without corrosive atmosphere. Afterwards, the weighed A3 carbon steel coupons were immersed in stone processing wastewater for 7 d, which contained different doses of BMN composite inhibitor with constant stirring at 200–250 rpm utilizing a agitator. After the 7 d immersion test, the carbon steel coupons were taken out and washed by deionized water and dried in room temperature. Finally, the carbon steel specimens were weighed with the accuracy of 0.0001 g [23].

2.4. Electrochemical experiments

Electrochemical measurements were conducted using a CS120 electrochemical workstation in a conventional three-electrode corrosion cell. The A3 carbon steel specimen, platinum electrode, and Ag/AgCl were used as the working electrode, counter electrode, and reference electrode, respectively. BMN composite inhibitor at concentrations of 0, 10, 20, 30, 40 and 50 $mL{\cdot}L^{-1}$ were added to the stone processing wastewater. The working surface area of A3 carbon steel is 1 cm^2. Electrochemical impedance spectroscopy (EIS) assessment was conducted in the frequency range 200 kHz~0.01 Hz with a single amplitude perturbation of 10 mV. Linear polarization resistance tests were performed within the potential range of OCP ± 10 mV with a scan rate of 5 mV/s [24,25].

Table 1
Characteristics of stone processing wastewater

pH	Total suspended solids	Conductivity	Turbidity
7.38	6,033.3 $mg{\cdot}L^{-1}$	4.91 $mS{\cdot}cm^{-1}$	4,920 NTU

2.5. Surface analysis

The morphology of the A3 carbon steel surface was observed using an scanning electron microscope (SEM, MIRA LMS, Tescan, Czech). The morphology measurement was conducted before and after immersing the specimens in stone processing wastewater without and with BMN composite inhibitor for 7 d.

3. Results and discussion

3.1. Measurement of weight loss

Weight losses and corresponding corrosion rates of stone processing wastewater with different dosage of BMN composite inhibitor to A3 carbon steel coupons for 7 d were measured (Fig. 1). The weight loss from specimens were adopted to calculate the inhibition efficiency (η) and corrosion rate (v). The relevant formulas are listed as follows [26,27]:

$$v = \frac{W_0 - W_1}{S \cdot t} \quad (1)$$

where W_0 and W_1 are the weight of the corresponding samples before and after the experiment (g), respectively, S is the steel surface area (cm^2), t is the immersion time (h).

$$\eta\% = \frac{v_1 - v_0}{v_0} \times 100 \quad (2)$$

where v_0 and v_1 are the corrosion rate ($g \cdot cm^{-2} \cdot h^{-1}$) of samples in inhibited and uninhibited solutions, respectively.

From Fig. 1, the rates of corrosion (v) of A3 carbon steel coupons decreased from 0.5833 to 0.0024 $g \cdot cm^{-2} \cdot h^{-1}$ and the corrosion inhibition efficiency (η) significantly increased from 48.16% to 99.59% with the increase of the concentration of BMN composite inhibitor. The inhibition efficiency (η) increased with higher BMN composite inhibitor concentrations, with a maximum inhibition efficiency of 99.59% at 50 $mL \cdot L^{-1}$, which was ascribed to an increase in the chemisorption of the BMN composite inhibitor on the carbon steel surface. In the experiment, A3 carbon steel coupons were pre-immersed in the BMN composite inhibitor solution to produce a protective film on the surface, and then the BMN composite inhibitor was added to the stone processing wastewater to form a thicker inhibitor layer through adsorption to block the contact between the samples and the corrosive medium. The inhibition efficiency of BMN composite inhibitor increased with the increase in the concentration of inhibitor.

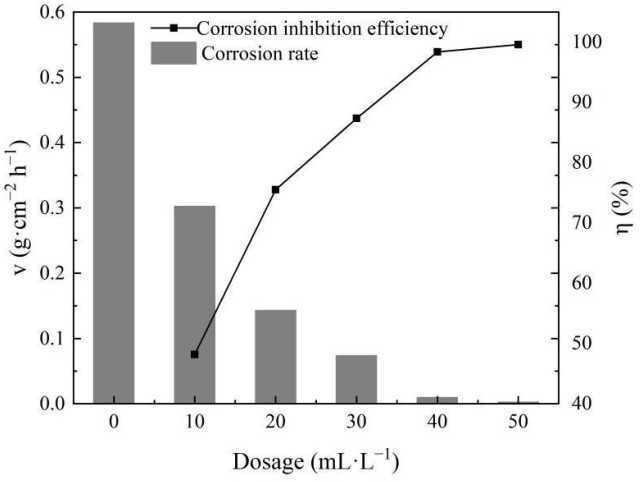

Fig. 1. Effect of BMN composite inhibitor dosage on inhibition effect.

3.2. Polarisation results

Fig. 2 depicts Tafel curves of the A3 carbon steel coupons in the stone processing wastewater with and without BMN composite inhibitor. The electrochemical parameters were characterized by corrosion potential (E_{corr}), current density (I_{corr}), anodic and cathodic Tafel slopes (β_a and β_c) [28]. The polarisation parameters in the presence and absence of BMN composite inhibitor are listed in Table 2. As shown in Fig. 2, the inhibitor pushed the current density towards

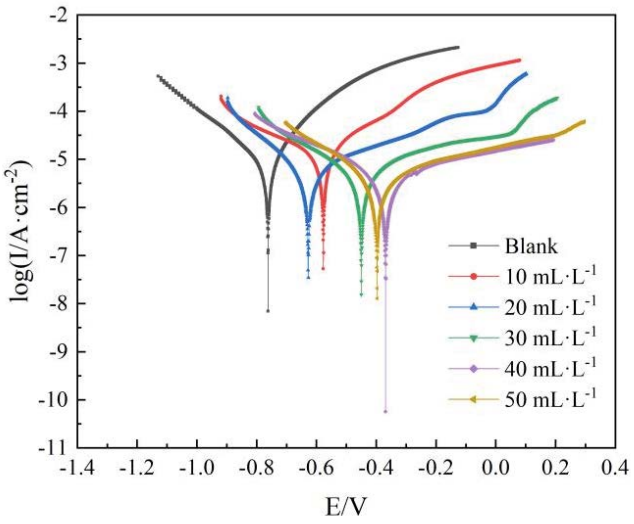

Fig. 2. Polarization curves of A3 carbon steel in stone processing wastewater with different concentrations of BMN composite inhibitor.

Table 2
Impedance parameter fitting of A3 carbon steel in stone processing wastewater with different concentrations of BMN composite inhibitor

c ($mL \cdot L^{-1}$)	β_a ($V \cdot dec^{-1}$)	β_c ($V \cdot dec^{-1}$)	E_{corr} (mV)	I_{corr} ($mA \cdot cm^{-2}$)	η_p (%)
0	0.15	0.24	–762	0.0279	–
10	0.47	0.56	–577	0.0210	24.73
20	1.10	0.33	–627	0.0209	25.09
30	1.18	0.51	–450	0.0194	30.47
40	2.63	0.66	–369	0.0108	61.29
50	2.70	0.52	–397	0.0057	79.57

lower values, which indicated that the addition of BMN composite inhibitor resulted in the inhibition of corrosion in carbon steel. And corrosion potential shifted towards the positive direction. According to the E_{corr}, it provided important information about the type of inhibitor. An inhibitor was considered as anodic or cathodic when the shift in corrosion potential between blank and inhibited systems was higher than ±85 mV [29]. Table 2 reveals that all shifts of approximately –400~–200 mV in the positive potential direction and there was irregular displacement in the E_{corr} values, similar behavior was previously observed in many others studies [30], which suggested that BMN composite inhibitor can be distinct as an anodic corrosion inhibitor [31].

The corrosion inhibition efficiencies (η_p, %) were calculated by the following equation [32]:

$$\eta_p\% = \frac{I_{corr_0} - I_{corr}}{I_{corr}} \times 100 \quad (3)$$

where I_{corr0} and I_{corr} represented the corrosion current densities in absence and presence of BMN composite inhibitor, respectively. By comparing the inhibition efficiencies determined by weight loss method (Fig. 1) and electrochemical tests (Table 2), it can be seen that after adding BMN composite inhibitor, the corrosion inhibition efficiencies measured by weight loss method were higher than those measured by electrochemical test. That is, after immersion in the BMN composite inhibitor solution, a protective film was formed on the surface of carbon steel, which further inhibited the corrosion reaction and reduced the corrosion inhibition efficiency.

3.3. Electrochemical impedance spectroscopy

EIS was an effective process to investigate the anti-corrosive characteristic of the inhibitor. Fig. 3a illustrates the Nyquist plots for A3 carbon steel in stone processing wastewater with and without different concentrations of BMN composite inhibitor at room temperature. As the BMN composite inhibitor concentration increased, the diameters of Nyquist plots also increased due to the resistance of charge transfer between the surface of the specimen and the corrosion medium was increasing constantly [29]. Fig. 3b illustrates the Bode plots for A3 carbon steel in stone processing wastewater with and without different concentrations of BMN composite inhibitor at room temperature. Generally, a low impedance modulus $|Z|_{0.01Hz}$ usually indicated severe corrosion [33,34]. The value of $|Z|_{0.01Hz}$ of A3 carbon steel coupons immersed in stone processing wastewater with the addition of the inhibitor 30 mL·L^{-1} was enhanced nearly an order of magnitude than that of without the addition of the inhibitor as shown in Fig. 3b, which indicated that the prepared BMN composite inhibitor exhibited outstanding anti-corrosion performance for saw blade corrosion in stone processing wastewater. Moreover, in the Nyquist plots of stone processing wastewater with 0, 10, and 20 mL·L^{-1} BMN composite inhibitor solution showed a single depressed semicircle, but with the BMN composite inhibitor concentration increasing, the second depressed capacitive was found, which indicated that a more complete protective film had formed on the surface of A3 carbon steel coupons [34].

Fig. 4 represents the equivalent circuit fitting in the absence (a) and the presence (b) of inhibitor. The impedance data of the stone processing wastewater without BMN composite inhibitor was fitted by the one–time constant electrical circuit model (Fig. 4a), while the two–time constant electrical circuit model (Fig. 4b) could be more suitable for the stone processing wastewater containing BMN composite inhibitor [35,36].

It should be noted that, where Rs was the solution resistance, CPE_1 and CPE_2 represented the capacitance of carbon steel surface films and the double electrical layer capacitance, respectively. R_2 and R_3 referred to resistance from the surface films and charge transfer resistance, respectively. The corresponding fitting parameters are listed in Table 3.

As shown in Table 3, with the concentration of BMN composite inhibitor increasing from 10 to 40 mL·L^{-1}, the R_2 increased from 1,844.2 to 9495.5 Ω·cm^{-2}, and the R_3 increased from 907.03 Ω·cm^{-2} to 2.481 × 10^{11} Ω·cm^{-2}, indicating that the corrosion was significantly suppressed, which also

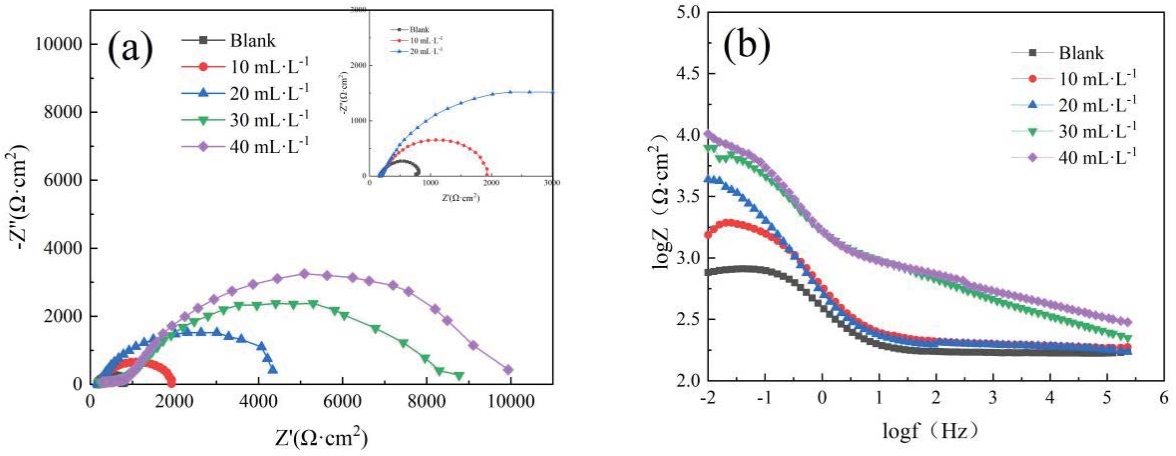

Fig. 3. Electrochemical impedance spectroscopy of A3 carbon steel in stone processing wastewater containing different concentrations of BMN inhibitor: (a) Nyquist plots and (b) Bode modulus plots.

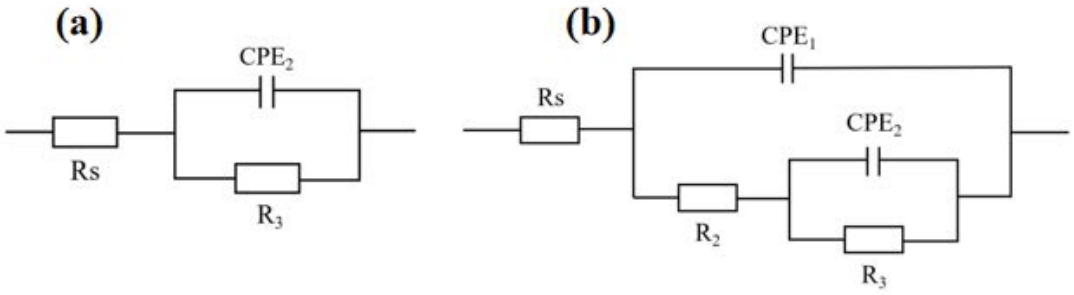

Fig. 4. Equivalent circuit fitting in the absence (a) and the presence (b) of inhibitor.

Table 3
Fitting results of electrochemical impedance spectroscopy parameters

c (mL·L^{-1})	Rs (Ω·cm^2)	R_2 (Ω·cm^2)	R_3 (Ω·cm^2)
0	168.55	–	651.74
10	203.22	1,844.2	907.03
20	196.16	4,502.8	5,053.2
30	870.40	7,430.5	3.9462×10^7
40	858.21	9,495.5	2.481×10^{11}

confirmed high efficiency of the inhibition performance of BMN composite inhibitor [27,36,37].

3.4. SEM observation

Fig. 5 presents the SEM morphological images of A3 carbon steel coupons after immersion in the solution in the absence and presence of BMN composite inhibitor for 7 d. Fig. 5a shows the surface of polished steel with deep and clear polishing scratches. There were severe corrosion on the sample surface without and with 20 mL·L^{-1} BMN composite inhibitor (Fig. 5b and c), which was attributed the corrosive

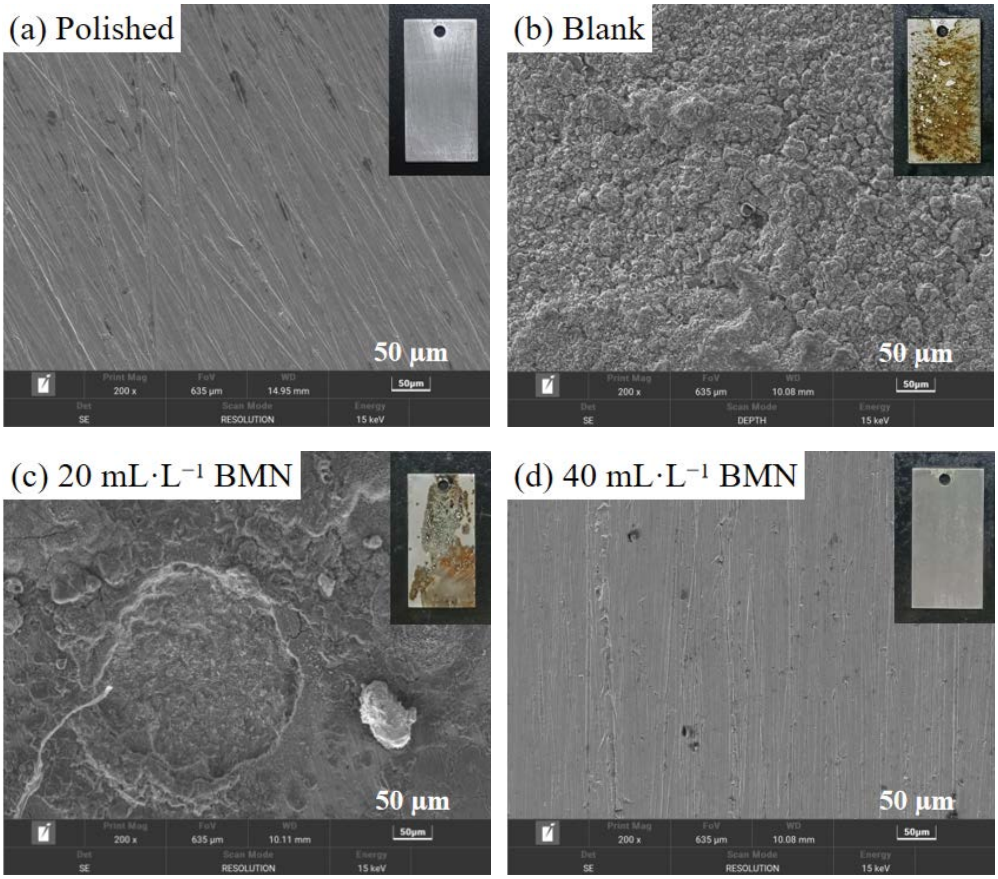

Fig. 5. Morphology of A3 carbon steel in stone processing wastewater: (a) polished metal sample, (b) blank, (c) A3 carbon steel sample immersed for 7 d in the presence of inhibitor at 20 mL·L^{-1} and (d) A3 carbon steel sample immersed for 7 d in the presence of inhibitor at 40 mL·L^{-1}.

effect of stone processing wastewater. While the A3 carbon steel surfaces in inhibited solution were improved (Fig. 5c), but local corrosion behavior such as pitting still existed. After the sample was immersed in 20 mL·L^{-1} BMN composite inhibitor solution, the much smoother surface without obvious corrosion products is displayed in Fig. 5d, which is similar to the image of polished steel. This further confirmed that the BMN composite inhibitor could form a very adherent and homogenous inhibitor layer on the surface of A3 carbon steel, thereby reducing metal's corrosion [38].

3.5. Comparison of inhibition efficiency

Table 4 summarizes the anti-corrosion properties of different metals treated with various organic corrosion inhibitors. Although the corrosion medium was different, the prepared BMN corrosion inhibitor still showed excellent corrosion inhibition efficiency on the easily corroded carbon steel materials in the high-salt stone processing wastewater.

3.6. Inhibition mechanism

Electrochemical corrosion is mainly divided into two categories: hydrogen evolution corrosion and oxygen corrosion [38,44]. Oxygen corrosion mainly occurs in neutral, weakly alkaline solutions, and the oxygen in the air will dissolve in the water, causing accelerated corrosion of the metal. In addition, the high conductivity of stone processing wastewater makes carbon steels more susceptible to corrosion. The above analysis indicates that the BMN composite inhibitor can restrain the corrosion of carbon steel by forming a protective film on the surface. As shown in Fig. 6, a possible corrosion mechanism of A3 carbon steel in stone processing wastewater could be expressed as the following reactions:

$$Fe \rightarrow Fe^{2+} + 2e^{-} \quad (4)$$

$$2H_2O + O_2 + 4e^{-} \rightarrow 4OH^{-} \quad (5)$$

$$2Fe + 2H_2O + O_2 \rightarrow 2Fe(OH)_2 \quad (6)$$

The Fe^{2+} was mainly produced by the oxidation reaction of carbon steel at the anode [Eq. (4)], while the OH^- was from the cathodic oxygen reduction reactions [Eq. (5), and the total corrosion reaction of carbon steel can be described as [Eq. (6)]. The O_2 in those reactions came from the dissolved

Table 4
Comparison of metal corrosion inhibition efficiency of various corrosion inhibitors

Inhibitors	Metals	Corrosion medium	Concentration	Inhibition efficiency	References
Methylbenzotriazole	Cu	DI water	15 mM	92.01%	[39]
TAZ				95.34%	
2,2′-[[(5-methyl-1H-benzotriazol-1-yl) methyl]imino]bisethanol	Cu	0.15 wt.% Gly + 0.5 wt.% H_2O_2	5 wt.%	99.90%	[40]
Benzotriazole	Pure Cu	DI water	1,000 ppm	95%	[41]
	Cu-60Ag			80.7%	
	Cu-6Ag			96.4%	
3,3′-Dithiodipropionic acid	Co	0.15 wt.% NH_4Cl + 0.5 wt.% H_2O_2	0.5 wt.%	90%	[42]
2,2′-Dibenzamidodiphenyl disulfide				84.8%	
Benzothiadiazole	Cu	3.5 wt.% NaCl	5 g·L^{-1}	53.67%	[43]
Benzimidazole				95.32%	
BMN	Carbon steel	Stone processing wastewater	50 mL·L^{-1}	99.59%	This work

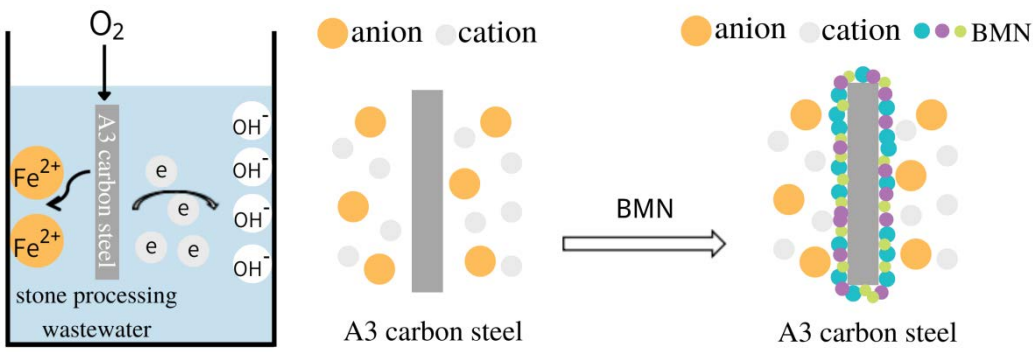

Fig. 6. Corrosion mechanism of A3 carbon steel in stone processing wastewater.

O_2 in the solution, which had great significance for the final corrosion products, such as Fe_2O_3 and Fe_3O_4. The existence of iron oxide protective film on the metal surfaces plays a key role in controlling metal corrosion [45].

The corrosion reaction was remarkably suppressed after adding BMN composite inhibitor into the corrosion medium. That is, BTA could interact with Fe^{2+} to form complexes, which then shaped a denser protective film on the surface of carbon steel to inhibit corrosion reactions. Meanwhile, sodium benzoate and sodium nitrite were anode corrosion inhibitors, both of them could form a protective film on the metal surface by adsorption [20]. Especially, nitrite could generate insoluble oxides on the surface of carbon steel in alkaline conditions. Although these single components formed a protective film on the surface of carbon steel through adsorption or chemical deposition, the prepared BMN composite inhibitor could better play the synergistic role of each component, the adsorbed combined inhibitor films could more efficaciously prevent the A3 carbon steel corrosion.

4. Conclusion

The BMN composite inhibitor was used as a corrosion inhibitor in stone processing wastewater for A3 carbon steel surface by using various techniques like gravimetric analysis, electrochemical measurements, and surface morphological studies. The following conclusions were drawn based on the findings:

- A new composite inhibitor BMN was synthesized by mixing BTA, sodium nitriazole, sodium nitrite, sodium molybdate, sodium silicate, triethanolamine and sodium benzoate at the mass ratio of 1:75:15:15:20:50, and the inhibition efficiency of BMN composite inhibitor was found to be 99.59% at 50 $mL \cdot L^{-1}$ in stone processing wastewater for A3 carbon steel.
- Polarization studies and electrochemical impedance spectroscopy indicated that BMN acted as anode inhibitor.
- The surface analysis demonstrated that BMN composite inhibitor could effectively inhibit the A3 carbon steel corrosion.

Declarations

Credit authorship contribution statement

Jingjing Xiang: Conceptualization, Writing-original draft, Formal analysis and Investigation. Hao Peng: Investigation, Methodology. Likun Li: Investigation, Methodology and Funding acquisition. Heng Liu: Investigation and Validation. Qiaoyun Zhu: Investigation. Yanjun Huang: Methodology. Yi Wang: Investigation and Formal analysis. Guozhi Fan: Investigation. Lei Zhang: Formal analysis, Investigation, Methodology, Funding acquisition, Project administration. All authors read and approved the final manuscript.

Availability of data and materials

All data generated or analyzed during this study are presented within the submitted manuscript.

Competing interests

The authors declare that they have no known competing financial interests or personal relationships that could have appeared to influence the work reported in this paper.

Funding

This work was supported by the Research and Innovation Initiatives of WHPU (Grant No. 2022Y16), the Scientific Research Foundation of Wuhan Polytechnic University (Grant No. 118-53210052171, 118-53210052144 and 118-53210052136) and the National Key Research and Development Program of China (Grant No. 2020YFE0205300).

Acknowledgements

The authors would like to thank Chengzhang Liu from Shiyanjia Lab (www.shiyanjia.com) for the SEM analysis.

References

[1] J. Cui, Y. Yang, X. Li, W. Yuan, Y. Pei. Towards a slow-release borate inhibitor to control mild steel corrosion in simulated recirculating water, ACS Appl. Mater. Interfaces., 10 (2018) 4183–4197.
[2] C. Jing, B. Dong, A. Raza, T. Zhang, Y. Zhang, Corrosion inhibition of layered double hydroxides for metal-based systems, Nano Mater. Sci., 3 (2021) 47–67.
[3] X. Wen, P. Bai, B. Luo, S. Zheng, C. Chen, Review of recent progress in the study of corrosion products of steels in a hydrogen sulphide environment, Corros. Sci., 139 (2018) 124–140.
[4] Y. Wang, Z. Yang, H. Hu, J. Wu, M. Finšgar, Indolizine quaternary ammonium salt inhibitors: the inhibition and anti-corrosion mechanism of new dimer derivatives from ethyl acetate quinolinium bromide and n-butyl quinolinium bromide, Colloids Surf., A, 651 (2022) 129649, doi: 10.1016/j.colsurfa.2022.129649.
[5] C. Gao, X. Zhao, P. Fatehi, X. Dong, K. Liu, S. Chen, S. Wang, F. Kong, Lignin copolymers as corrosion inhibitor for carbon steel, Ind. Crops Prod., 168 (2021) 113585, doi: 10.1016/j.indcrop.2021.113585.
[6] W. Zhang, C. Li, W. Wang, B. Li, X. Liu, Y. Liu, H. Guo, S. Chen, Y. Feng, Laminarin and sodium molybdate as efficient sustainable inhibitor for Q235 steel in sodium chloride solution, Colloids Surf., A, 637 (2022) 128199, doi: 10.1016/j.colsurfa.2021.128199.
[7] I.A. Annon, A.S. Abbas, W.K. Al-Azzawi, M.M. Hanoon, A.A. Alamiery, W.N.R.W. Isahak, A.A.H. Kadhum, Corrosion inhibition of mild steel in hydrochloric acid environment using thiadiazole derivative: weight loss, thermodynamics, adsorption and computational investigations, S. Afr. J. Chem. Eng., 41 (2022) 244–252.
[8] A.A. Ayoola, R. Babalola, B.M. Durodol, E.E. Alagbe, O. Agboola, E.O. Adegbile, Corrosion inhibition of A36 mild steel in 0.5 M acid medium using waste *Citrus limonum* peels, Results Eng., 15 (2022) 100490, doi: 10.1016/j.rineng.2022.100490.
[9] A. Pal, C. Das, A novel use of solid waste extract from tea factory as corrosion inhibitor in acidic media on boiler quality steel, Ind. Crops Prod., 151 (2020) 112468, doi: 10.1016/j.indcrop.2020.112468.
[10] H. Zhang, L. Zhao, D. Liu, J. Wang, X. Zhang, C. Chen, Early period corrosion and scaling characteristics of ductile iron pipe for ground water supply with sodium hypochlorite disinfection, Water Res., 176 (2020) 115742, doi: 10.1016/j.watres.2020.115742.
[11] C.U.D. Eze, N.A. Madueke, N.B. Iroha, N.J. Maduelosi, L.A. Nnanna, V.C. Anadebe, A.A. Chokor, Adsorption and

inhibition study of N-(5-methoxy-2-hydroxybenzylidene) isonicotinohydrazide Schiff base on copper corrosion in 3.5% NaCl, Egypt. J. Pet., 31 (2022) 31–37.
[12] W. Guo, M. Talha, Y. Lin, X. Kong, Schiff's base with center of symmetry as an effective corrosion inhibitor for mild steel in acid medium: electrochemical & simulation studies, Colloids Surf., A, 615 (2021) 126234, doi: 10.1016/j.colsurfa.2021.126234.
[13] M. Turano, M. Walker, F. Grillo, C. Gattinoni, G. Hunt, P. Kirkman, N.V. Richardson, C.J. Baddeley, G. Costantini, Adsorption of the prototypical organic corrosion inhibitor benzotriazole on the Cu(100) surface, Corros. Sci., 207 (2022) 110589, doi: 10.1016/j.corsci.2022.110589.
[14] I.B. Onyeachu, M.M. Solomon, Benzotriazole derivative as an effective corrosion inhibitor for low carbon steel in 1 M HCl and 1 M HCl + 3.5 wt.% NaCl solutions, J. Mol. Liq., 313 (2020) 113536, doi: 10.1016/j.molliq.2020.113536.
[15] M.A. Osipenko, D.S. Kharytonau, A.A. Kasach, J. Ryl, J. Adamiec, I.I. Kurilo, Inhibitive effect of sodium molybdate on corrosion of AZ31 magnesium alloy in chloride solutions, Electrochim. Acta, 144 (2022) 140175, doi: 10.1016/j.electacta.2022.140175.
[16] D. Wang, M. Wu, J. Ming, J. Shi, Inhibitive effect of sodium molybdate on corrosion behaviour of AA6061 aluminium alloy in simulated concrete pore solutions, Constr. Build. Mater., 270 (2021) 121463, doi: 10.1016/j.conbuildmat.2020.121463.
[17] J.K. Das, B. Pradhan, Effect of sodium nitrite on chloride-induced corrosion of steel in concrete, Mater. Today Proc., 65 (2022) 636–643.
[18] A. Mohamed, D.P. Visco Jr., D.M. Bastidas, Effect of cations on the activity coefficient of NO_2^-/NO_3^- corrosion inhibitors in simulated concrete pore solution: an electrochemical thermodynamics study, Corros. Sci., 206 (2022) 110476, doi: 10.1016/j.corsci.2022.110476.
[19] M. Kaseem, M.P. Kamil, J.H. Kwon, Y.G. Ko, Effect of sodium benzoate on corrosion behavior of 6061 Al alloy processed by plasma electrolytic oxidation, Surf. Coat. Technol., 283 (2015) 268–273.
[20] T. Zheng, L. Wang, J. Liu, J. Wang, G. Jia, The corrosion inhibition effect of sodium silicate and Triton X-100 on 2024-T3 aluminum alloy in NaOH medium: experimental and theoretical research, Colloids Surf., A, 610 (2021) 125723, doi: 10.1016/j.colsurfa.2020.125723.
[21] C. Wang, J. Chen, B. Hu, Z. Liu, C. Wang, J. Han, M. Su, Y. Li, C. Li, Modified chitosan-oligosaccharide and sodium silicate as efficient sustainable inhibitor for carbon steel against chloride-induced corrosion, J. Cleaner Prod., 238 (2019) 117823, doi: 10.1016/j.jclepro.2019.117823.
[22] L.B. Coelho, M. Lukaczynska-Anderson, S. Clerick, G. Buytaert, S. Lievens, H.A. Terryn, Corrosion inhibition of AA6060 by silicate and phosphate in automotive organic additive technology coolants, Corros. Sci., 199 (2022) 110188, doi: 10.1016/j.corsci.2022.110188.
[23] V. Saraswat, M. Yadav, Improved corrosion resistant performance of mild steel under acid environment by novel carbon dots as green corrosion inhibitor, Colloids Surf., A, 627 (2021) 127172, doi: 10.1016/j.colsurfa.2021.127172.
[24] D. Wang, C. Yang, M.A. Saleh, M.D. Alotaibi, M.E. Mohamed, D. Xu, T. Gu, Conductive magnetite nanoparticles considerably accelerated carbon steel corrosion by electroactive *Desulfovibrio vulgaris* biofilm, Corros. Sci., 205 (2022) 110440, doi: 10.1016/j.corsci.2022.110440.
[25] D. Wang, Y. Li, T. Chang, A. Luo, Experimental and theoretical studies of chitosan derivatives as green corrosion inhibitor for oil and gas well acid acidizing, Colloids Surf., A, 628 (2021) 127308, doi: 10.1016/j.colsurfa.2021.127308.
[26] M. Rbaa, M. Ouakki, M. Galai, A. Berisha, B. Lakhrissi, C. Jama, I. Warad, A. Zarrouk, Simple preparation and characterization of novel 8-hydroxyquinoline derivatives as effective acid corrosion inhibitor for mild steel: experimental and theoretical studies, Colloids Surf., A, 602 (2020) 125094, doi: 10.1016/j.colsurfa.2020.125094.
[27] O.M.A. Khamaysa, I. Selatnia, H. Lgaz, A. Sid, H. Lee, H. Zeghache, M. Benahmed, I.H. Ali, P. Mosset, Hydrazone-based green corrosion inhibitors for API grade carbon steel in HCl: insights from electrochemical, XPS, and computational studies, Colloids Surf., A, 626 (2021) 127047, doi: 10.1016/j.colsurfa.2021.127047.
[28] M. Galai, M. Rbaa, H. Serrar, M. Ouakki, A. Ech-chebab, A.S. Abousalem, E. Ech-chihbi, K. Dahmani, S. Boukhris, A. Zarrouk, M. EbnTouhami, S-Thiazine as effective inhibitor of mild steel corrosion in HCl solution: synthesis, experimental, theoretical and surface assessment, Colloids Surf., A, 613 (2021) 126127, doi: 10.1016/j.colsurfa.2020.126127.
[29] N.P. Swathi, S. Samshuddin, A.H. Alamri, K. Rasheeda, V.D.P. Alva, T.A. Aljohani, Experimental and theoretical investigation of a new triazole derivative for the corrosion inhibition of carbon steel in acid medium, Egypt. J. Pet., 31 (2022) 15–21.
[30] Z.R. Farag, M.E. Moustapha, E.H. Anouar, G.M.A. El-Hafeez, The inhibition tendencies of novel hydrazide derivatives on the corrosion behavior of mild steel in hydrochloric acid solution, J. Mater. Res. Technol., 16 (2022) 1422–1434.
[31] M.A. Bidi, M. Azadi, M. Rassouli, A new green inhibitor for lowering the corrosion rate of carbon steel in 1 M HCl solution: *Hyalomma* tick extract, Mater. Today Commun., 24 (2020) 100996, doi: 10.1016/j.mtcomm.2020.100996.
[32] Y. Zhang, Y. Pan, P. Li, X. Zeng, B. Guo, J. Pan, L. Hou, X. Yin, Novel Schiff base-based cationic Gemini surfactants as corrosion inhibitors for Q235 carbon steel and printed circuit boards, Colloids Surf., A, 623 (2021) 126717, doi: 10.1016/j.colsurfa.2021.126717.
[33] E. Li, J. Wu, D. Zhang, P. Wang, L. Zhu, C. Li, Z. Sun, Y. Gao, Effect of autoinducer-2 on corrosion of Q235 carbon steel caused by sulfate reducing bacteria, Corros. Sci., 200 (2022) 110220, doi: 10.1016/j.corsci.2022.110220.
[34] G. Salinas-Solano, J. Porcayo-Calderon, L.M. Martinez de la Escalera, J. Canto, M. Casales-Diaz, O. Sotelo-Mazon, J. Henao, L. Martinez-Gomez, Development and evaluation of a green corrosion inhibitor based on rice bran oil obtained from agro-industrial waste, Ind. Crops Prod., 119 (2018) 111–124.
[35] M.H. Johar, H. Torbati-Sarraf, M. Ahangari, M. Saremi, Inhibiting effect of Benzotriazole on the stress corrosion cracking of Cu-27%Ni cupronickel and Cu-30%Zn brass in Mattsson's solution, Mater. Lett., 293 (2021) 129735, doi: 10.1016/j.matlet.2021.129735.
[36] P.E. Alvarez, M.V. Fiori-Bimbi, R.V. Valenti, J.R. Hidalgo, S.A. Brand´an, C.A. Gervasi, Improved electrochemical strategy to characterize adsorption and corrosion inhibition related to biomolecules from plant extracts: The case of *Annona cherimola*, Results Chem., 4 (2022) 100233, doi: 10.1016/j.rechem.2021.100233.
[37] A. Cruz-Zabalegui, E. Vazquez-Velez, G. Galicia-Aguilar, M. Casales-Diaz, R. Lopez-Sesenes, J.G. Gonzalez-Rodriguez, L. Martinez-Gomez, Use of a non-ionic Gemini-surfactant synthesized from the wasted avocado oil as a CO_2^- corrosion inhibitor for X-52 steel, Ind. Crops Prod., 133 (2019) 203–211.
[38] L. Košeka, L. Rozumová, A. Hojná, C. Aparicio, M. Vronka, J. Vít, Mechanism of localized corrosion issues of austenitic steels exposed to flowing lead with 10^{-7} wt.% oxygen at 480°C up to 16,000 h, J. Nucl. Mater., 572 (2022) 154045, doi: 10.1016/j.jnucmat.2022.154045.
[39] D. Yin, L. Yang, B. Tan, T. Ma, S. Zhang, Y. Wang, L. Guo, B. Gao, Y. He, Theoretical and electrochemical analysis on inhibition effects of benzotriazole derivatives (un- and methyl) on copper surface, J. Mol. Struct., 1243 (2021) 130871, doi: 10.1016/j.molstruc.2021.130871.
[40] T. Ma, B. Tan, Y. Xu, D. Yin, G. Liu, N. Zeng, G. Song, Z. Kao, Y. Liu, Corrosion control of copper wiring by barrier CMP slurry containing azole inhibitor: combination of simulation and experiment, Colloids Surf., A, 599 (2020) 124872, doi: 10.1016/j.colsurfa.2020.124872.
[41] H. Rahmani, E.I. Meletis, Corrosion study of brazing Cu–Ag alloy in the presence of benzotriazole inhibitor, Appl. Surf. Sci., 497 (2019) 143759, doi: 10.1016/j.apsusc.2019.143759.
[42] T. Ma, B. Tan, L. Guo, W. Wang, W. Li, J. Ji, M. Yan, S. Kaya, Experimental and theoretical investigation on the inhibition performance of disulfide derivatives on cobalt corrosion in

alkaline medium, J. Mol. Liq., 341 (2021) 116907, doi: 10.1016/j.molliq.2021.116907.
[43] H. Huang, X. Guo, The relationship between the inhibition performances of three benzo derivatives and their structures on the corrosion of copper in 3.5 wt.% NaCl solution, Colloids Surf., A, 598 (2020) 124809, doi: 10.1016/j.colsurfa.2020.124809.
[44] W. Zhang, D. Zhang, X. Li, C. Li, L. Gao, Excellent performance of dodecyl dimethyl betaine and calcium gluconate as hybrid corrosion inhibitors for Al alloy in alkaline solution, Corros. Sci., 207 (2022) 110556, doi: 10.1016/j.corsci.2022.110556.
[45] C. Yu, M. Zhang, F. Xu, L. Meng, Y. Wei, Y. Chang, M. Zhang, D. Fu, H. Wang, A multiple synergistic composite coating with ultrahigh anti-corrosion performance under harsh oxygen environment, Corros. Sci., 208 (2022) 110696, doi: 10.1016/j.corsci.2022.110696.